analytical chemistry

Open Access
This article is licensed under CC-BY-NC-ND 4.0

pubs.acs.org/ac
Article

One-Step Immunoassay for Biomarker Quantification in Complex Mixtures Based on Phase-Separated Antifouling Coacervates

Philippe S. Lenzen, Tobias Hoch, Itzel Condado-Morales, Raphaël P. B. Jacquat, Roberto Frigerio, Jonathan Garlipp, Francesca Torrini, Alessandro Gori, Umberto Capasso Palmiero, Onur Boyman, and Paolo Arosio*

Cite This: *Anal. Chem.* 2025, 97, 4906−4914
Read Online

ACCESS | Metrics & More | Article Recommendations | Supporting Information

ABSTRACT: We develop and present a one-pot sandwich immunoassay (termed oneSTEP) to detect target biomolecules in complex biological fluids based on programmable zwitterionic polymer coacervates. We design these coacervates to selectively recruit target analytes with ultralow nonspecific adsorption. We show that dynamic compartmentalization combined with local target enrichment delivers a rapid and wash-free sandwich immunoassay with high specificity and a high signal-to-noise ratio. The fluorescence-based readout is performed using standard microscopy methods and flow cytometry. We demonstrate the capabilities of the oneSTEP assay by detecting complement component 5 in human serum and the spike protein of severe acute respiratory syndrome coronavirus 2 in artificial saliva with a limit of detection of 300 pM. The results highlight the potential of the oneSTEP sandwich immunoassay as complementary to bead-based approaches in high-throughput screening studies as well as clinical diagnostics.

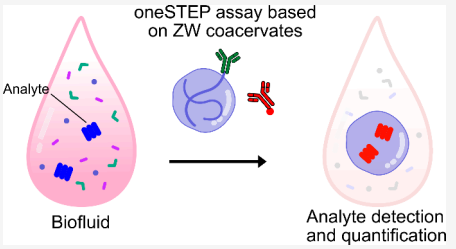

INTRODUCTION

Rapid identification and quantification of disease-related protein biomarkers are central to understanding molecular mechanisms of diseases, monitoring disease progression, and guiding personalized treatment strategies.[1−3] Immunoassay techniques that rely on specific interactions between antibodies and antigens have demonstrated their strength in diagnostics.[4−6] Specifically, heterogeneous immunoassays, which require physical separation of antibody-bound antigen from free antigen, remain the preferred option for diagnostic applications.[7] However, the numerous liquid handling steps necessary for separation and subsequent washing increase the time required for analysis and the potential for errors during the assay procedure. To reduce time, variability, and handling errors, these assays are often implemented in combination with automated liquid handling techniques, ranging from high-throughput pipetting robots[8] to microfluidic formats.[9,10] However, such automation can increase the complexity of assay development and the costs of assay implementation. Consequently, novel technologies providing simple user operation and fast readout times, while maintaining the high specificity and flexibility of heterogeneous immunoassays, constitute an important goal in the field of immunoassays.

Isolation methods based on polymeric coacervates represent promising candidates for the development of immunoassays.[11−16] Coacervates are obtained via phase separation of polymers in solution, leading to the formation of a dense polymer phase surrounded by a polymer-depleted phase.[17−21] The dense phase often appears as liquid-like compartments in the micrometer-size range dispersed in aqueous solution. The properties of the coacervates, such as polymer concentration, size distribution, and material properties, can be tuned by modulating intermolecular interactions that govern the phase separation, for instance, by changing environmental stimuli such as ionic strength, temperature, and pH.[22,23] Coacervates can recruit and localize "client" molecules in their interiors, providing a means for the physical separation required by heterogeneous assays. Moreover, as they lack a membrane, this exchange and recruitment of molecules from the dilute phase are highly dynamic. The combination of spontaneous phase separation and dynamic exchange of molecular analytes within a benign liquid-like environment makes these coacervates an ideal approach for the development of novel immunoassay applications.

The application of polymeric coacervates for diagnostic applications can be challenging due to the significant issue of biofouling. This nonspecific adsorption of proteins and other components found in biological matrices can decrease the sensitivity, accuracy, and reliability of diagnostic assays.[24] To tackle this nonspecific adsorption problem, researchers have generated various polymeric fouling-resistant materials.[25−31]

Received: August 30, 2024
Revised: February 3, 2025
Accepted: February 11, 2025
Published: February 27, 2025

ACS Publications
© 2025 The Authors. Published by American Chemical Society

https://doi.org/10.1021/acs.analchem.4c04661
Anal. Chem. 2025, 97, 4906−4914

Recently, our group developed stimuli-responsive coacervates based on zwitterionic polymers that undergo phase separation under a broad range of ionic strengths, temperatures, and pH values, including conditions typically found in biological samples.[32] Importantly, these coacervates exhibit excellent antifouling properties due to the pairing of charged groups and the strong hydration shell around the positive and negative charges.[33] Thus, these coacervates have the key ability to exclude most molecules and exhibit ultralow nonspecific binding, even in complex biological matrices. Starting from this reference material, selective capture and recruitment of target biomolecules into coacervates can be programmed by suitable functionalization of the polymer. This can be achieved by promoting electrostatic interactions by the functionalization of the polymer with charged groups[34] or through affinity interactions by conjugation of the polymer with an affinity-tag.[32]

Here, we apply these polymeric coacervates to develop an innovative sandwich immunoassay diagnostic platform, which we term a one-pot Selective Target Enrichment by Polymer (oneSTEP) immunoassay. Selective recruitment of the target analyte into the coacervate is achieved by affinity capture by coupling the zwitterionic polymers with an antibody, followed by detection by the addition of a fluorescently labeled detection antibody. We demonstrate that the sandwich immunoassay can be performed in complex mixtures with high sensitivity and selectivity without the need for separation and washing steps. We illustrate the capabilities of the oneSTEP assay by detecting the presence of relevant biomarkers, including the quantification of the spike protein of severe acute respiratory syndrome coronavirus 2 (SARS-CoV-2) in a saliva mimic and measurement of complement component 5 (C5) in human serum. The latter target is a central molecule of the complement system and has recently been used to identify persistent Long Covid disease.[35]

EXPERIMENTAL SECTION

Materials. The following materials were used for spike detection in saliva: artificial saliva for pharmaceutical research (Sigma-Aldrich, US), SARS-CoV-2 antispike antibody MM43, antibody CR3022, and recombinant Spike protein (Sino Biologicals, CN), HRP antimouse IgG, TMB substrate, and stop solutions for ELISA (Abcam, US). The following materials were used for complement C5 detection in serum: Human C5-depleted serum (Sigma-Aldrich, US), Human C5 Antibody Pair (Abcam, US), C5 protein isolated and purified from human serum (Sigma-Aldrich, US), and biotin rabbit IgG isotype control (Abcam, US). The following materials were used for polymer synthesis: *N*-(3-sulfopropyl)-*N*-methacryloxyethyl-*N*,*N*-dimethylammonium betaine (SB, Sigma-Aldrich, US), 4,4′-azobis(4-cyanovaleric acid) (ACVA, Sigma-Aldrich, US), 4-cyano-4-(phenylcarbonothioylthio) pentanoic acid (CPA, Sigma-Aldrich, US), 2-hydroxyethyl methacrylate (HEMA, Sigma-Aldrich, US), and mono-2-(methacryloyloxy) ethyl succinate (HEMA-succinate, Sigma-Aldrich, US). The monomer sulfabetaine methacrylate (ZB) was synthesized according to a previously described protocol.[36] The following materials were used for polymer conjugation: *N*-Hydroxysuccinimide (NHS, Carl Roth, DE), *N*-(3-(Dimethylamino)-propyl)-*N*′-ethylcarbodiimide hydrochloride (EDC, Sigma-Aldrich, US), and streptavidin from streptomyces avidinii (Sigma-Aldrich, US). The following materials were used for the immunoassay: tween 20 (Sigma-Aldrich, US), bovine serum albumin (BSA, Sigma-Aldrich, US, and Ester Technopole, FR), MagnaBind carboxyl derivatized beads (ThermoFisher Scientific, US). Additionally, urine samples collected from pooled donors (Lee Biosolutions, USA) were used for polymer characterization.

Clinical Samples and Ethics Statement. The collection of human serum samples was approved by the Cantonal Ethics Committee of Zurich (BASEC #2016-01440). Following venous blood sampling, BD Vacutainer CAT serum tubes (Becton Dickinson, Franklin Lakes, NJ) were centrifuged at 1100*g* and 4 °C for 10 min. Upon centrifugation, serum was stored at −80 °C until analysis.

Polymer Synthesis. The zwitterionic copolymers synthesized in this study are composed of two monomers: sulfabetaine methacrylate (ZB) acting as the "sticker", and sulfobetaine methacrylate (SB) acting as the "spacer". Two copolymers with two different compositions were used in this study: a zwitterionic copolymer composed of ZB and SB monomers, designated here as "ZW" (DP_{ZB} = 130, DP_{SB} = 70), and a second polymer chain, indicated at "ZWSucc" (DP_{ZB} = 140, DP_{SB} = 60, $DP_{HEMA\text{-}Succinate}$ = 5), containing additional carboxylic groups from mono-2-(methacryloyloxy) ethyl succinate (HEMA-Succinate) to increase the number of functional groups available for antibody conjugation. The synthesis of ZW and ZWSucc copolymers was performed by Reversible Addition−Fragmentation chain Transfer (RAFT) polymerization following a previously described protocol using 4,4′-azobis(4-cyanovaleric acid) (ACVA) as an initiator and 4-cyano-4-(phenylcarbonothioylthio) pentanoic acid (CPA) as a RAFT agent[32] (characterization of the polymer can be found in Figure S1).

Polymer Conjugation and Antibody Labeling. The polymer conjugation to the antibody was performed via an amide coupling reaction using 1-ethyl-3-(3-(dimethylamino)-propyl) carbodiimide (EDC) and *N*-hydroxysuccinimide (NHS). For quantification of the spike protein in saliva, ZWSucc polymer was conjugated to the anti-S capture antibody via direct coupling. Ten milligrams of ZWSucc, 3 mg of EDC, and 5 mg of NHS were dissolved in 215 μL of MES buffer (0.1 M MES, 1 M NaCl, pH 6.0) and stirred at room temperature for 15 min. The pH was subsequently raised to 8.2 with 1 M Na_2CO_3 and 50 μL of antibody at 1 mg/mL was added. The mixture was stirred gently at room temperature for 1 h. Subsequently, the mixture was diluted in 30 mL of deionized water and kept at 4 °C for 2 h to promote phase separation. The solution was subsequently centrifuged at 4600*g* for 30 min. The supernatant was discarded, and the pellet containing the zwitterionic polymer was resuspended in 600 mM NaCl to achieve a final polymer concentration of 40 mg/mL. The conjugated polymer was stored at 4 °C for up to a year without loss of activity.

For the quantification of C5 in serum, the ZW polymer was first coupled to streptavidin using the same NHS-EDC procedure described above and with the addition of 10 mg/mL of streptavidin. Biotinylation of the antibody was performed using an EasyLink quick biotinylation kit (Abcam, US) following the manufacturer's protocol. Conjugation of the antibody to the streptavidin-conjugated polymer was performed by incubating for 2 h a solution of 20 mg/mL ZW polymer and 250 nM biotinylated-capture antibody in 600 mM NaCl (the characterization of the conjugation step can be found in Figures S2−S4).

https://doi.org/10.1021/acs.analchem.4c04661
Anal. Chem. 2025, 97, 4906−4914

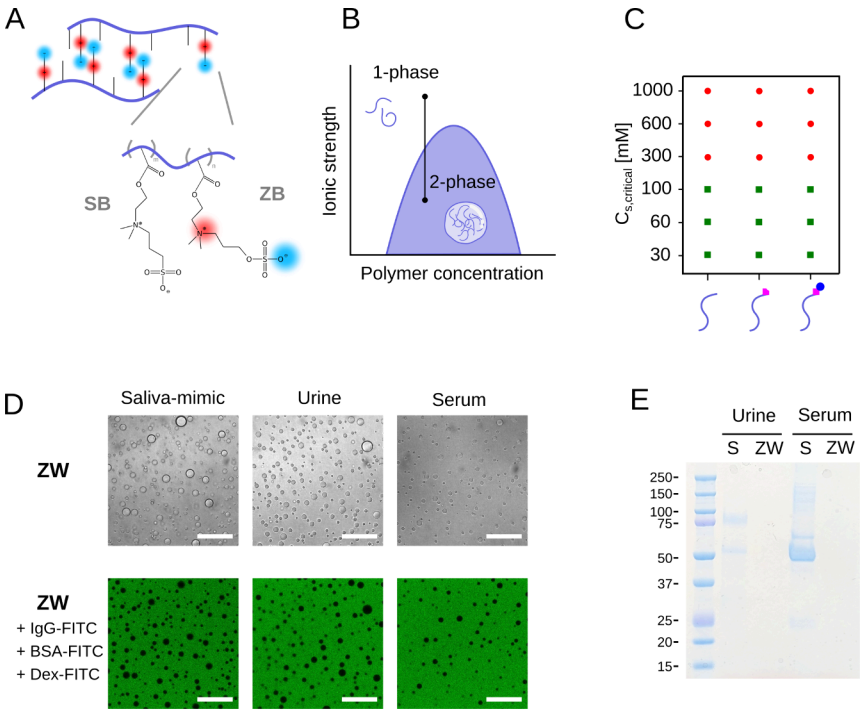

Figure 1. Properties of zwitterionic polymer coacervates. (A) Chemical structure of the zwitterionic polymer composed of the monomers sulfabetaine methacrylate (ZB) (acting as a sticker) and sulfobetaine methacrylate (SB). (B) Schematic phase diagram of the polymer as a function of the salt concentration. Phase separation was induced by reducing the ionic strength of the stock homogeneous solution. (C) Phase diagram of the polymer as a function of salt concentration with and without conjugation with an affinity-tag and in the absence and presence of its target. Red circles and green squares indicate absence and presence of phase separation, respectively. (D) Brightfield and fluorescence microscopy images of the polymer coacervates formed in synthetic saliva (saliva-mimic), human urine, or human serum in the presence of labeled IgG, BSA and 10 kDa dextran at a concentration of 1 μM. Fluorescence images demonstrate the antifouling property of the zwitterionic coacervates. Scale bar represents 50 μm. (E) SDS-Page analysis of protein content in the supernatant (S) and dense polymer phase (ZW) in urine and serum after 2 h of incubation. Supernatant and dense phases were separated by centrifugation. Serum supernatant was diluted 1:200 prior to running the SDS-Page to ensure efficient band separation.

Antibody labeling with an AlexaFluor 647 fluorescent dye was performed using an EasyLink quick labeling kit (Abcam, US) following the manufacturers protocol.

oneSTEP Immunoassay Workflow. A sixteen microliter portion of the sample was added to an individual well of 384 μL in a multiwell plate. Two microliters of the polymer conjugated to a capture antibody (at 20 mg/mL in 600 mM NaCl) and 2 μL of the fluorescently labeled detection antibody (at a final concentration of 1 nM) were added to the sample and incubated for 1 h. The fluorescence signal within the coacervates was then quantified by using either confocal microscopy or flow cytometry.

Confocal Microscopy Detection of Spike Protein in Saliva Mimic. Detection of the SARS-CoV-2 spike protein in a saliva mimic was performed using confocal microscopy imaging to monitor the fluorescence signal of the secondary antibodies recruited in the polymer coacervates. To facilitate imaging and prevent wetting of the coacervates at the glass bottom of the multiwell plate, a BSA coating was performed by incubating a 10 mg/mL BSA solution for 30 min prior to the assay.

A dilution series of the spike protein (S) from 100 nM to 10 pM in synthetic saliva containing 0.5% BSA was measured in duplicate. As controls, saliva-mimic alone and a dilution series analyzed using a nonconjugated polymer were also measured.

Imaging was performed using a spinning disk confocal microscope (Leica SP8, DE). Images were acquired in both the *XY* and *XZ* planes using a 63x oil objective. Quantification of the fluorescence intensity was performed using Image J (NIH, US) by analysis of the *XZ* plane images acquired close to the glass bottom of the microplate, with an average of 3 individual coacervates analyzed per image. The total fluorescence signal of the coacervates was obtained by averaging 3 replicates (more details can be found in the Supporting Information).

Flow Cytometry Detection of Complement C5 in Serum. To prevent wetting of the coacervates at the bottom of the multiwell plate, a BSA coating was performed by incubating a blocking buffer (PBS with 20 mg/mL BSA and 0.1% Tween-20) overnight at 4 °C prior to the assay. Human serum and C5-depleted serum aliquots were thawed and diluted 1:10 in assay buffer (PBS, 0.1% Tween-20, and 1% BSA). C5-depleted serum was supplemented with human C5 at a concentration of 40 nM. A dilution series was prepared using an assay buffer. Subsequently, 25 μL of the sample was mixed with 25 μL of polymer solution in a 96-well plate. The solution contained 2.5 μL of polymer conjugated to a capture antibody or an isotype antibody (at 20 mg/mL in 600 mM NaCl) and 0.5 μL of fluorescently labeled detection antibody (at 1000 nM) diluted in PBS.

The sample-polymer mix was incubated for 1 h and protected from light. Upon incubation, samples were further diluted in 200 μL of assay buffer and immediately acquired on a Cytek Aurora spectral flow cytometer. Flow cytometry data were analyzed by using FlowJo (version 10.9.0). Of all recorded events, particles within a certain size range were selected for export (Figure S5). Debris, very small particles,

https://doi.org/10.1021/acs.analchem.4c04661
Anal. Chem. 2025, 97, 4906−4914

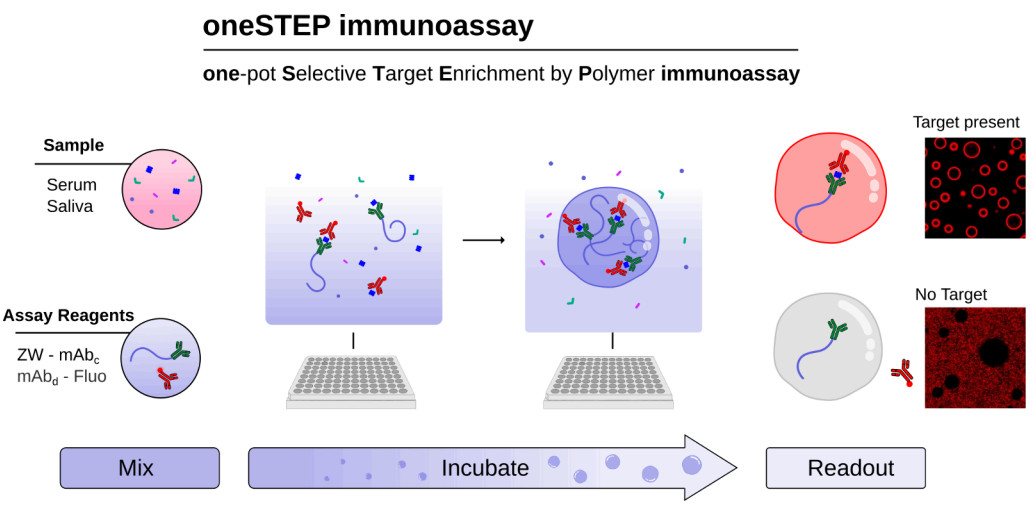

Figure 2. Schematic representation of the workflow of the oneSTEP immunoassay.

and free polymers were excluded from the analysis. All samples were analyzed by using the same gate. Of the gated events, the top 10% fraction with the highest signal intensity of every sample was selected for analysis. Data were subsequently analyzed and visualized using GraphPad software (Dotmatics, US).

Bead-Based Immunoassay for the Detection of Complement C5. Carboxyl magnetic beads were functionalized with streptavidin in accordance with the manufacturer's protocol. Streptavidin beads were subsequently incubated with biotinylated antibodies anti-C5 or isotype controls for 1 h under orbital shaking at room temperature. C5-depleted serum aliquots were thawed and diluted 1:20 in assay buffer (PBS, 0.1% Tween-20, 1% BSA), and supplemented with human C5 at a concentration of 20 nM. A dilution series was prepared in an assay buffer.

Antibody-functionalized beads were diluted in assay buffer (PBS, 0.1% Tween-20, 1% BSA) to obtain a stock with a final bead concentration of 10^8 beads/mL. Ten microliters of bead stock was washed for each condition in assay buffer (PBS, 0.1% Tween-20, 1% BSA), and subsequently incubated with the relevant samples for 1 h, 800 rpm at 25 °C. Following this incubation period, the beads were subjected to three consecutive separation and washing steps using 300 μL of assay buffer. Hundred microliters of anti-C5 detection antibody labeled with AF647 were incubated for 1 h at 800 rpm at 25 °C. Following the final incubation, the beads were washed three times, resuspended in 0.5 mL of assay buffer, and analyzed by flow cytometry on a CytoFLEX S system (Beckman Coulter).

RESULTS AND DISCUSSION

Principle of the oneSTEP Immunoassay. The oneSTEP immunoassay presented here is based on the programmable and dynamic phase separation of zwitterionic polymers in aqueous solutions. The polymer is composed of two monomer units. Sulfabetaine methacrylate (ZB) acts as a "sticker" and promotes the attractive paired ion−ion interactions responsible for the simple coacervation, whereas sulfobetaine methacrylate (SB) serves as a "spacer" and further modulates the solubility of the polymer (Figure 1A). The phase separation of this zwitterionic polymer is enthalpy-driven and exhibits upper critical solution temperature behavior (UCST), i.e., coacervation is promoted at lower temperature values[32] and low ionic strength (Figure 1B). In this assay, the polymer was originally stored in a homogeneous solution at a high salt concentration, which screens the attractive electrostatic interactions. Upon mixing the stock solution with the sample, the decrease of the ionic strength of the solution induced phase separation.

Three key aspects described below were demonstrated to be essential to the successful operation of the immunoassay. First, the polymer is functionalized with an affinity tag capable of capturing the biomarker of interest in the polymer-rich coacervates. The use of monoclonal antibodies as affinity tags ensures the high specificity required for accurate identification of the biomarker, as it minimizes the cross-reactivity with nontarget molecules. In addition, the formation of an antibody−antigen complex on the polymer, followed by its recruitment into the coacervates, enables target quantification through the formation of a sandwich immunoassay complex occurring in the coacervates. In this work, we functionalized the polymer through the formation of a covalent amide bond between the carboxyl group on the polymer chain and the amine group on the conjugation target through NHS-EDC chemistry (more details in Materials and Methods). Importantly, we verified that the phase separation behavior of the zwitterionic polymer is independent of either its conjugation to an affinity tag or binding to the target (Figure 1C). This is critical since the correct implementation of the assay requires binding to the target in the dilute phase, followed by recruitment in the dense phase. A change in the phase separation behavior would lead to a higher concentration of the polymer-target complex in the dilute phase and therefore be detrimental to the correct quantification of the concentration of the target biomarker.

Second, because of the selective recruitment and compartmentalization in polymer-rich coacervates, the described material locally concentrates the target biomarker. When combined with an efficient readout of detection, this improves the signal-to-noise ratio and therefore the limit of detection of the method, which can be crucial in the case of targets of low abundance. The ability to enhance the signal, without the need for any preliminary sample preparation or additional amplification steps, is a key feature of the oneSTEP immunoassay.

https://doi.org/10.1021/acs.analchem.4c04661
Anal. Chem. 2025, 97, 4906−4914

Third, polymer compartmentalization generates an interface between the polymer-rich coacervates and the bulk solution. As is the case for heterogeneous immunoassays, this surface can be prone to nonspecific adsorption of proteins from the sample matrix, which can be detrimental to accurate biomarker quantification. As a result, workflows of surface-based immunoassays are often centered on effective surface washing to avoid biofouling and nonspecific signals. However, due to the pairing of the charged groups and the zwitterionic nature of the polymer chains, the resulting interface of the coacervates exhibits a hydration shell that limits the nonspecific adsorption of biomolecules and confers a strong antifouling effect on this material.[37] Here, we demonstrate the antifouling property of the zwitterionic polymer even in complex mixtures. To this aim, we analyzed by fluorescence microscopy coacervates formed in synthetic saliva, human urine, and human serum in the presence of a mixture of fluorescently labeled IgG, BSA, and dextran. We observed the fluorescent signal only in the dilute phase, thereby demonstrating the strong antifouling property of the coacervates even in complex mixtures (Figure 1D). Additionally, we formed zwitterionic coacervates in both urine and serum and, using SDS-Page analysis, compared the protein content in the coacervates (ZW) and the dilute phase (Figure 1E, more details can be found in the Supporting Information). The results demonstrate that the coacervates contained no detectable protein, highlighting their ultralow nonspecific adsorption, thus eliminating the need for washing steps in the oneSTEP immunoassay.

As a result of the properties of the zwitterionic polymer coacervates, the workflow of the assay is greatly simplified compared to that of other heterogeneous immunoassay techniques. An assay mixture composed of polymer functionalized with a capture antibody specific to a target (ZW-mAb$_c$), and a fluorescently labeled detection antibody (mAb$_d$-Fluo), are mixed with the sample of interest (Figure 2). This single step is followed by an hour-long incubation, during which the polymer will compartmentalize into polymer-rich coacervates in which the formation of the sandwich immunoassay complex can be observed by the fluorescence signal.

Conjugated polymer is mixed with the nonconjugated polymer at a ratio of 1:400. Since the polymer-antibody conjugate has higher hydrophilicity compared to the polymer, the polymer coacervates form a mesoscale architecture in which a nonconjugated polymer core is surrounded by an outer shell of the conjugated polymer. Consequently, the fluorescent signal is localized on the outer shell of the coacervates surrounding the nonfunctionalized polymer core (Figure 2).

Validation of oneSTEP Assay for SARS-CoV-2 Spike Protein Detection in Saliva Mimic. We first applied our assay to quantify the concentration of SARS-CoV-2 spike (S) protein in a saliva mimic. For this purpose, a serial dilution of S protein in a concentration range between 10 pM and 100 nM was performed in artificial saliva. Samples were mixed with polymer conjugated to a capture antibody (ZWSucc-CR3022), followed by a fluorescently labeled detection antibody (MM43-AF647). The use of these two antibodies as an appropriate antibody pair for a sandwich immunoassay was validated by ELISA measurements (more details can be found in the Supporting Information and Figure S6).

In the absence of antigen, the polymer coacervates did not exhibit fluorescence, and most of the signal represented background fluorescence (Figure 3A, 0 nM). On the contrary,

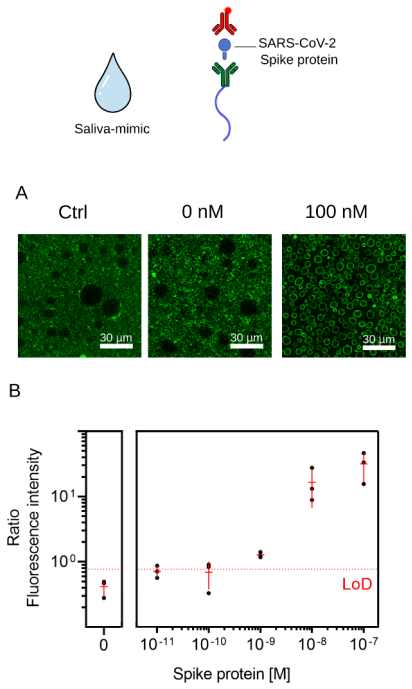

Figure 3. SARS-CoV-2 spike protein quantification in synthetic saliva. Clones CR3022 and MM43 were used as capture and detection antibody, respectively. (A) Confocal microscopy images of samples in the absence (0 nM) and presence (100 nM) of spike protein, as well as of a control ("Ctrl") with nonconjugated polymer and 100 nM spike protein. (B) Fluorescence intensity of polymer coacervates as a function of spike protein concentration. The limit of detection (LoD) of 0.75 nM is indicated by a dashed red line.

at high S protein concentration (100 nM), a fluorescence signal localized at the rim of the functionalized coacervates was observed (Figure 3A, 100 nM). This localized fluorescence signal was absent in control coacervates lacking functionalization (Figure 3A). This result confirmed the recruitment of the S protein and demonstrated the expected formation of the sandwich immunoassay complex composed of a capture antibody, S protein, and detection antibody.

Analysis of the fluorescence signal within coacervates resulted in a dose–response curve (Figure 3B; details on evaluation intensity in Materials and Methods). At low antigen concentration, the fluorescence signal was comparable to background noise, while an increase of S protein concentration in the saliva-mimic correlated with an increase in coacervate fluorescence. Following the guidelines provided by the Clinical and Laboratory Standards Institute,[38] a limit of detection of 0.75 nM was calculated for this assay.

Flow Cytometry Detection of Complement C5 in Human Serum. After demonstrating the potential of our oneSTEP immunoassay for quantification of an analyte in synthetic saliva, we aimed to expand the capabilities of the assay and apply the approach to detect biomarkers in serum, where the increase in matrix complexity requires strong antifouling capabilities. Due to its reported role in identifying individuals with active Long Covid, C5 was selected as the target of our investigations.[35]

While S protein detection was performed using confocal microscopy, we decided to use flow cytometry-based quantification of the coacervates in order to increase experimental throughput. The resulting methodology enabled the quantification of 30 samples per hour, thus markedly

https://doi.org/10.1021/acs.analchem.4c04661
Anal. Chem. 2025, 97, 4906−4914

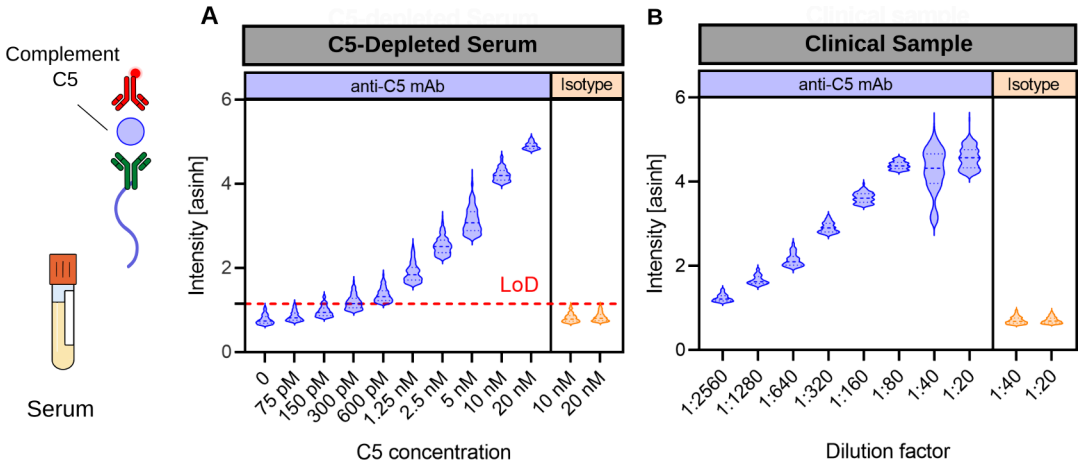

Figure 4. oneSTEP immunoassay for complement component 5 (C5) quantification in serum using flow cytometry. (A) Dilution series of C5 between 0 and 20 nM in C5-depleted serum. Quantification of droplet fluorescence using flow cytometry demonstrated an LoD of approximately 300 pM. (B) Quantification of C5 in a human serum sample by serial dilution from 1:20 to 1:2560. The highest C5 concentrations for both C5-depleted serum and clinical samples were analyzed using a polymer conjugated to an isotype control antibody to demonstrate the specificity of the assays.

improving the potential of the assay and enabling its use in facilities where throughput is required.

Moreover, to increase the flexibility of the assay, instead of directly coupling the ZW polymer with an antibody, the polymer was functionalized with streptavidin and mixed with the biotinylated anti-C5 antibody. This functionalization enabled the rapid and simple conjugation of the polymer to any biotinylated antibody.

Quantification of C5 in diluted serum (1:20 dilution) was initially performed by a serial dilution of C5 in C5-depleted serum in a concentration range between 0 and 20 nM. These samples were mixed with polymer conjugated with capture antibody (ZW-mAb$_c$) and fluorescently labeled detection antibody (mAb$_d$-AF647). A dose−response was observed, exhibiting the highest signal at the highest C5 concentration (Figure 4A). Measurements of samples with the highest C5 concentration (10 and 20 nM) were also performed using a polymer conjugated to an isotype control to characterize the specificity of the assay. Fluorescence intensity values of the isotype control were similar to the intensities observed for the blank condition (C5-depleted serum), thus demonstrating the specificity of the assay and the absence of nonspecific binding to polymer coacervates. The limit of detection of the assay was calculated to be approximately 300 pM for this measurement, demonstrating that the assay allowed the quantification of C5 in serum with the required sensitivity for diagnostic application.

To show the potential of the oneSTEP platform in diagnostic use, we performed the same analysis to quantify C5 in a clinical serum sample, for which the normal range of C5 concentration was between 300 and 600 nM.[39,40] The dilution series from 1:20 until 1:2560 exhibited a good dose−response with a linear correlation from 1:80 to 1:2560, and no fluorescent signal in the isotype control (Figure 4B). These results demonstrate the capabilities of oneSTEP immunoassay for biomarker quantification in clinically relevant samples.

The antifouling properties of the zwitterionic coacervates play a key role in achieving the observed low limit of detection without any washing step. To highlight this aspect, we quantified C5 in C5-depleted serum using a magnetic bead immunoassay format, in which the material was not optimized to prevent nonspecific adsorption in complex mixtures. To this end, magnetic beads were functionalized with the anti-C5 capture antibody, and the readout was performed with the same anti-C5 detection antibody used in the coacervate assay. The coated beads were incubated with the relevant samples for 2 h for antigen capture, followed by a magnetic separation step and three times washing. Subsequently, the antigen-bound beads were incubated for another 2 h with the detection anti-C5 antibody, followed by another separation and washing step. After these steps, the beads were resuspended in a buffer, and the fluorescence intensity was quantified using a flow cytometer. The fluorescence intensity of anti-C5 conjugated magnetic beads increased with increasing C5 concentration, displaying a dose−response comparable to the quantification performed with the oneSTEP immunoassay (Figure 5). However, at high target concentrations, the beads conjugated to the isotype control exhibited substantial fluorescence intensity, indicative of significant nonspecific adsorption to the surface of the magnetic beads. Consequently, the quantifiable target concentration with the bead-based immunoassay is approximately 1 order of magnitude higher than the limit of detection using the oneSTEP immunoassay.

Moreover, compared to the oneSTEP immunoassay, quantification of C5 using bead-based methodologies required significantly more user input and four times longer time. This extended workflow originated from the series of stringent and laborious steps of incubation, separation, and washing, which were needed to minimize nonspecific adsorption to the surface of beads. The nonspecific adsorption of the zwitterionic coacervates simplified the protocol of the oneSTEP immunoassay, minimizing not only the analysis time but also the potential for error, thus increasing the reliability of the assay.

CONCLUSIONS

In this work, we developed a novel oneSTEP immunoassay based on the coacervation of phase separating zwitterionic polymers,[32,34,41] which exhibited a series of key features for immunoassay diagnostics. First, we demonstrated that the zwitterionic polymer phase separated in all major biological fluids, including saliva, urine, and serum, and that its phase separation behavior was not affected by the conjugation of the

https://doi.org/10.1021/acs.analchem.4c04661
Anal. Chem. 2025, 97, 4906−4914

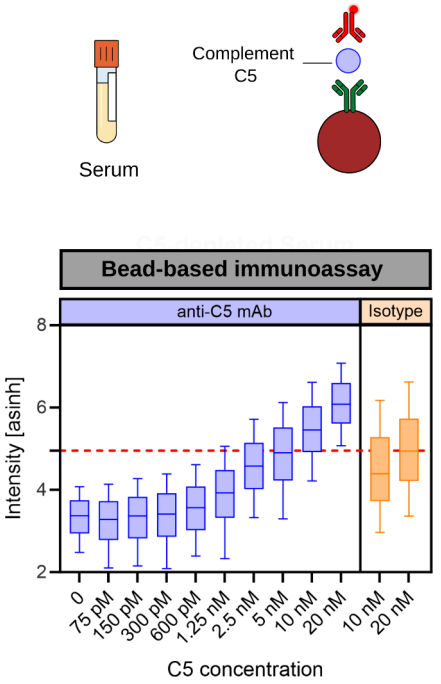

Figure 5. Quantification of C5 spiked in C5-depleted serum using bead-based methodologies. Dilution series of C5 between 0 and 20 nM in C5-depleted serum measured using an anti-C5 antibody. The two highest C5 concentrations were also measured using an isotype control, which highlights the high nonspecific fluorescence signal.

polymer. As a result, the oneSTEP assay has the flexibility to be implemented for applications involving all of the major diagnostically relevant biofluids.

Moreover, we demonstrated the excellent antifouling characteristic of the zwitterionic polymer in these three complex biological matrices. This antifouling behavior provides a great benefit to tackle nonspecific adsorption of molecules that affects most heterogeneous immunoassays, as was illustrated by comparing the quantification of C5 using the zwitterionic coacervates and magnetic beads as an assay support. In the latter case, the high nonspecific adsorption of molecules to the bead surface resulted in higher fluorescent signal intensity in the isotype control, while quantification of C5 using the oneSTEP assay provided a limit of detection close to 300 pM.

Importantly, the polymer's antifouling abilities allow the development of an immunoassay without the need for separation and washing steps. This one-pot approach enables biomarker quantification without user intervention, in contrast to traditional heterogeneous immunoassay techniques, where each separation and washing step is prone to error and can lead to the wrong target quantification. As a result, the oneSTEP approach offers reliable and efficient immunoassay analysis.

Our study also shows that the novel oneSTEP immunoassay is compatible with existing high-throughput methodologies, as demonstrated by the quantification of C5 using flow cytometry. Enabling the measurement of approximately 30 individual conditions per hour without the need for additional sample processing results in a significant reduction of time and processing requirements, while remaining compatible with standard readout techniques used in bead-based immunoassays.

Further improvements are necessary to enhance the effectiveness and applicability of the oneSTEP immunoassay. In particular, replacing antibodies with more stable and cost-effective binders, such as peptides or aptamers, could provide benefits in terms of stability and scalability, making the system more suitable for a wider range of applications. Additionally, enhancing the sensitivity of the assay for early detection or detection of low abundance compounds could be achieved through further optimization of the assay conditions and refinement of the readout technique.

In conclusion, this work highlights a novel diagnostic approach in which zwitterionic polymer coacervates were employed for their compartmentalization and dynamic recruitment of biomarkers in biological fluids. We demonstrate their power in a sandwich immunoassay in complex mixtures, offering high sensitivity and selectivity without the need for separation or washing steps. This work emphasizes the potential of the oneSTEP immunoassay approach as an alternative to bead-based assays in high-throughput screening studies, as well as clinical diagnostics.

■ ASSOCIATED CONTENT

Supporting Information

The Supporting Information is available free of charge at https://pubs.acs.org/doi/10.1021/acs.analchem.4c04661.

Characterization of polymer and polymer conjugation; ^{1}H-NMR spectra of the zwitterionic polymers; SEC-HPLC analysis of polymer conjugation; UV absorbance spectrum of the zwitterionic polymers; fluorescence intensity measurements of zwitterionic polymers; gating strategy used for the flow cytometry detection of the oneSTEP immunoassay; and ELISA for spike detection (PDF)

■ AUTHOR INFORMATION

Corresponding Author

Paolo Arosio − *Department of Chemistry and Applied Biosciences, Swiss Federal Institute of Technology Zurich, 8093 Zurich, Switzerland*; Email: paolo.arosio@chem.ethz.ch

Authors

Philippe S. Lenzen − *Department of Chemistry and Applied Biosciences, Swiss Federal Institute of Technology Zurich, 8093 Zurich, Switzerland*; orcid.org/0009-0006-4543-0268

Tobias Hoch − *Department of Immunology, University Hospital Zurich, University of Zurich, 8091 Zurich, Switzerland*; orcid.org/0000-0003-0319-6064

Itzel Condado-Morales − *Department of Chemistry and Applied Biosciences, Swiss Federal Institute of Technology Zurich, 8093 Zurich, Switzerland*

Raphaël P. B. Jacquat − *Department of Chemistry and Applied Biosciences, Swiss Federal Institute of Technology Zurich, 8093 Zurich, Switzerland*

Roberto Frigerio − *Department of Chemistry and Applied Biosciences, Swiss Federal Institute of Technology Zurich, 8093 Zurich, Switzerland; Consiglio Nazionale delle Ricerche, Istituto di Scienze e Tecnologie Chimiche "Giulio Natta" (SCITEC), 20133 Milan, Italy*

https://doi.org/10.1021/acs.analchem.4c04661
Anal. Chem. 2025, 97, 4906−4914

Jonathan Garlipp − *Department of Chemistry and Applied Biosciences, Swiss Federal Institute of Technology Zurich, 8093 Zurich, Switzerland*
Francesca Torrini − *Department of Chemistry and Applied Biosciences, Swiss Federal Institute of Technology Zurich, 8093 Zurich, Switzerland*
Alessandro Gori − *Consiglio Nazionale delle Ricerche, Istituto di Scienze e Tecnologie Chimiche "Giulio Natta" (SCITEC), 20133 Milan, Italy;* orcid.org/0000-0003-1640-7238
Umberto Capasso Palmiero − *Department of Chemistry and Applied Biosciences, Swiss Federal Institute of Technology Zurich, 8093 Zurich, Switzerland*
Onur Boyman − *Department of Immunology, University Hospital Zurich, University of Zurich, 8091 Zurich, Switzerland; Faculty of Medicine and Faculty of Science, University of Zurich, 8091 Zurich, Switzerland*

Complete contact information is available at: https://pubs.acs.org/10.1021/acs.analchem.4c04661

Notes

The authors declare the following competing financial interest(s): U.C.P. and P.A. have filed PCT/EP2021/084452 patent application titled "Programmable polymer droplets and associated uses".

■ ACKNOWLEDGMENTS

This work was supported by the Swiss National Science Foundation (CRSII5-189950). The authors would like to thank ScopeM (ETH Zurich) for their support and assistance in this work, in particular Dr. Tobias Schwarz.

■ REFERENCES

(1) Yager, P.; Domingo, G. J.; Gerdes, J. *Annual Review of Biomedical Engineering.* **2008**, *10*, 107.
(2) World Health Organization *First WHO Model List of Essential In Vitro Diagnostics*; World Health Organization, 2019.
(3) Dinnes, J.; Deeks, J. J.; Berhane, S.; Taylor, M.; Adriano, A.; Davenport, C.; Dittrich, S.; Emperador, D.; Takwoingi, Y.; Cunningham, J.; Beese, S.; Domen, J.; Dretzke, J.; Ferrante di Ruffano, L.; Harris, I. M.; Price, M. J.; Taylor-Phillips, S.; Hooft, L.; Leeflang, M. M. G.; McInnes, M. D. F.; Spijker, R.; Van den Bruel, A.; Arevalo-Rodriguez, I.; Buitrago, D. C.; Ciapponi, A.; Mateos, M.; Stuyf, T.; Horn, S.; Salameh, J. P.; McGrath, T. A.; van der Pol, C. B.; Frank, R. A.; Prager, R.; Hare, S. S.; Dennie, C.; Jenniskens, K.; Korevaar, D. A.; Cohen, J. F.; van de Wijgert, J.; Damen, J. A. A. G.; Wang, J.; Agarwal, R.; Baldwin, S.; Herd, C.; Kristunas, C.; Quinn, L.; Scholefield, B. *Cochrane Database Syst. Rev.* **2020**, *8*, No. CD013705.
(4) Darwish, I. A. *Int. J. Biomed. Sci.* **2006**, *2*, 217−235.
(5) Li, Z.; Yi, Y.; Luo, X.; Xiong, N.; Liu, Y.; Li, S.; Sun, R.; Wang, Y.; Hu, B.; Chen, W.; Zhang, Y.; Wang, J.; Huang, B.; Lin, Y.; Yang, J.; Cai, W.; Wang, X.; Cheng, J.; Chen, Z.; Sun, K.; Pan, W.; Zhan, Z.; Chen, L.; Ye, F. *J. Med. Virol.* **2020**, *92* (9), 1518.
(6) Carter, L. J.; Garner, L. V.; Smoot, J. W.; Li, Y.; Zhou, Q.; Saveson, C. J.; Sasso, J. M.; Gregg, A. C.; Soares, D. J.; Beskid, T. R.; Jervey, S. R.; Liu, C. *ACS Cent. Sci.* **2020**, *6* (5), 591.
(7) Wild, D. *The Immunoassay Handbook: Theory and Applications of Ligand Binding, ELISA and Related Techniques*; Oxford, **2013**.
(8) Torres-Acosta, M. A.; Lye, G. J.; Dikicioglu, D. *Biochem. Eng. J.* **2022**, *188*, No. 108713.
(9) Volpetti, F.; Garcia-Cordero, J.; Maerkl, S. J. *PLoS One* **2015**, *10* (2), No. e0117744.
(10) Yafia, M.; Ymbern, O.; Olanrewaju, A. O.; Parandakh, A.; Sohrabi Kashani, A.; Renault, J.; Jin, Z.; Kim, G.; Ng, A.; Juncker, D. *Nature* **2022**, *605* (7910), 464.
(11) Auditore-Hargreaves, K.; Houghton, R. L.; Monji, N.; Priest, J. H.; Hoffman, A. S.; Nowinski, R. C. *Clin. Chem.* **1987**, *33* (9), 1509−1516.
(12) Hoffman, J. M.; Stayton, P. S.; Hoffman, A. S.; Lai, J. J. *Bioconjugate Chem.* **2015**, *26* (1), 29.
(13) Monji, N.; Hoffman, A. S. *Appl. Biochem. Biotechnol.* **1987**, *14*, 107−120.
(14) Kim, J. Y.; O'Malley, S.; Mulchandani, A.; Chen, W. *Anal. Chem.* **2005**, *77* (8), 2318.
(15) Zhu, Q. Z.; Liu, F.; Xu, J. G.; Su, W.; Huang, J. *Analyst* **1998**, *123* (5), 1131.
(16) Zhou, J.; Cai, Y.; Wan, Y.; Wu, B.; Liu, J.; Zhang, X.; Hu, W.; Cohen Stuart, M. A.; Wang, J. *J. Colloid Interface Sci.* **2023**, *650*, 2065.
(17) Sing, C. E.; Perry, S. L. *Soft Matter.* **2020**, *16* (12), 2885−2914.
(18) Rubinstein, M.; Colby, R. H. *Polymer Physics*; Oxford University Press, 2003.
(19) Banani, S. F.; Lee, H. O.; Hyman, A. A.; Rosen, M. K. *Nature Reviews Molecular Cell Biology.* **2017**, *18*, 285.
(20) Dai, Y.; You, L.; Chilkoti, A. *Nat. Rev. Bioeng.* **2023**, *1* (7), 466.
(21) Mittag, T.; Pappu, R. V. *Mol. Cell* **2022**, *82*, 2201.
(22) Galaev, I.; Mattiasson, B. *SMART POLYMERS: Applications in Biotechnology and Biomedicine*; CRC Press, 2007.
(23) Brangwynne, C. P.; Tompa, P.; Pappu, R. V. *Nat. Phys.* **2015**, *11*, 899−904.
(24) Sturgeon, C. M.; Viljoen, A. *Ann. Clin. Biochem.* **2011**, *48*, 418.
(25) Chen, A.; Kozak, D.; Battersby, B. J.; Forrest, R. M.; Scholler, N.; Urban, N.; Trau, M. *Langmuir* **2009**, *25* (23), 13510.
(26) Statz, A. R.; Meagher, R. J.; Barron, A. E.; Messersmith, P. B. *J. Am. Chem. Soc.* **2005**, *127* (22), 7972.
(27) Maan, A. M. C.; Hofman, A. H.; de Vos, W. M.; Kamperman, M. *Adv. Funct. Mater.* **2020**, *30*, No. 2000936.
(28) Dalsin, J. L.; Messersmith, P. B. *Mater. Today* **2005**, *8*, 38−46.
(29) Shiddiky, M. J. A.; Kithva, P. H.; Kozak, D.; Trau, M. *Biosens. Bioelectron.* **2012**, *38* (1), 132−137.
(30) Chan, D.; Chien, J. C.; Axpe, E.; Blankemeier, L.; Baker, S. W.; Swaminathan, S.; Piunova, V. A.; Zubarev, D. Y.; Maikawa, C. L.; Grosskopf, A. K.; Mann, J. L.; Soh, H. T.; Appel, E. A. *Adv. Mater.* **2022**, *34* (24), No. e2109764.
(31) Sabaté del Río, J.; Henry, O. Y. F.; Jolly, P.; Ingber, D. E. *Nat. Nanotechnol.* **2019**, *14* (12), 1143.
(32) Capasso Palmiero, U.; Paganini, C.; Kopp, M. R. G.; Linsenmeier, M.; Küffner, A. M.; Arosio, P. *Adv. Mater.* **2022**, *34* (4), No. e2104837.
(33) Schlenoff, J. B. *Langmuir* **2014**, *30*, 9625.
(34) Paganini, C.; Capasso Palmiero, U.; Picciotto, S.; Molinelli, A.; Porello, I.; Adamo, G.; Manno, M.; Bongiovanni, A.; Arosio, P. *Small* **2023**, *19* (1), No. e2204736.
(35) Cervia-Hasler, C.; Brüningk, S. C.; Hoch, T.; Fan, B.; Muzio, G.; Thompson, R. C.; Ceglarek, L.; Meledin, R.; Westermann, P.; Emmenegger, M.; Taeschler, P.; Zurbuchen, Y.; Pons, M.; Menges, D.; Ballouz, T.; Cervia-Hasler, S.; Adamo, S.; Merad, M.; Charney, A. W.; Puhan, M.; Brodin, P.; Nilsson, J.; Aguzzi, A.; Raeber, M. E.; Messner, C. B.; Beckmann, N. D.; Borgwardt, K.; Boyman, O. *Science* **2024**, *383* (6680), No. eadg7942.
(36) Sponchioni, M.; Rodrigues Bassam, P.; Moscatelli, D.; Arosio, P.; Capasso Palmiero, U. *Nanoscale* **2019**, *11* (35), 16582.
(37) Chen, S.; Li, L.; Zhao, C.; Zheng, J. *Polymer* **2010**, *51*, 5283−5293.
(38) Clinical and Laboratory Standards Institute *Protocols for Determination of Limits of Detection and Limits of Quantitation; Approved Guideline. CLSI Document EP17-A*; Clinical and Laboratory Standards Institute, **2004**; Vol. *24*.
(39) Eichenberger, E. M.; Dagher, M.; Ruffin, F.; Park, L.; Hersh, L.; Sivapalasingam, S.; Fowler, V. G.; Prasad, B. C. *Eur. J. Clin. Microbiol. Infect. Dis.* **2020**, *39* (11), 2121.
(40) Skjeflo, E. W.; Brækkan, S. K.; Ludviksen, J. K.; Snir, O.; Hindberg, K.; Mollnes, T. E.; Hansen, J. B. *Blood* **2021**, *138* (21), 2129.

(41) Villois, A.; Capasso Palmiero, U.; Mathur, P.; Perone, G.; Schneider, T.; Li, L.; Salvalaglio, M.; deMello, A.; Stavrakis, S.; Arosio, P. *Small* **2022**, *18*, No. e2202606.

https://doi.org/10.1021/acs.analchem.4c04661
Anal. Chem. 2025, 97, 4906−4914